http://www.sjst.psu.ac.th

Original Article

Effects of orientation and density of thermoplastic polyurethane honeycomb print on impact response in footwear and absorption applications♣

Satta Srewaradachpisal[1, 4, 5*], Surapong Chatpun[2], Muhammad Nouman[3],
and Wiriya Thongruang[1, 4]

*[1] Department of Mechanical Engineering, Faculty of Engineering,
Prince of Songkla University, Hat Yai, Songkhla, 90112 Thailand*

*[2] Department of Biomedical Sciences and Biomedical Engineering, Faculty of Medicine,
Prince of Songkla University, Hat Yai, Songkhla, 90110 Thailand*

*[3] Sirindhorn School of Prosthetics and Orthotics, Faculty of Medicine,
Siriraj Hospital, Mahidol University, Bangkok Noi, Bangkok, 10700 Thailand*

*[4] Smart Industry Research Center, Department of Industrial and Manufacturing Engineering, Faculty of Engineering,
Prince of Songkla University, Hatyai Campus, Songkhla, 90110 Thailand*

*[5] Center of Excellence in Metal and Materials Engineering,
Prince of Songkla University, Songkhla, 90110 Thailand*

Abstract

This study examined how 3D printing might increase impact force reduction in footwear application. The study used 3D honeycomb constructions of thermoplastic polyurethane to show how print orientation and density affect footwear's sensitivity to impact energy. Thorough characterization and standardized testing were used to analyze 3D-printed honeycomb lattice mechanical properties. This showed that construction orientation and density affect stiffness and elasticity. The fundamental investigation in this study revolved around the crucial relationship between construction orientation and density, which affects impact force dissipation. The transverse structure exhibited the highest impact reduction efficiency of 0.75 in our analysis, whereas the alternative structures only managed 0.65. Conversely, the impact reduction was significantly more influenced by the appropriate structural density than by the orientation angle. Impact mitigation and absorption applications can be better accommodated through the use of 3D honeycomb TPU printing, which enables manufacturers to create comfortable protection.

Keywords: 3D printing TPU, impact force, footwear, hip-protector, honeycomb orientation angle

1. Introduction

The impact forces experienced during physical activities can significantly affect the health and comfort of individuals wearing shoes (Mercer & Horsch, 2015; O'Leary *et al*., 2008; Price *et al*., 2014; Silva *et al*., 2009). Insufficient absorption and mitigation of these forces by footwear can lead to discomfort, fatigue, and even prolonged injuries. To address this concern, footwear manufacturers have been incorporating specialized functions and technologies into their products to enhance impact protection (Dib *et al*., 2005; O'Leary *et al*., 2008; Silva *et al*., 2009).

One crucial component responsible for cushioning in footwear is the midsole, which plays a vital role in reducing the impact forces transmitted to the feet and lower extremities. Traditional materials used in midsole production include Ethylene-vinyl acetate (EVA), polyurethane (PU) foam, and other elastic materials (Brückner *et al*., 2010; Heidenfelder *et al*., 2009; Lippa *et al*., 2014; Silva *et al*., 2009; Speed *et al*., 2018; Verdejo & Mills, 2004). These materials must possess certain essential features, such as effective impact reduction and being lightweight.

While traditional manufacturing methods limit the creation of complex internal structures in shoe soles, three-dimensional (3D) printing technology has emerged as a promising solution. 3D printing has revolutionized the manufacturing industry, enabling the production of diverse products with varying properties such as hardness, compressive strength, and energy absorption (Bates *et al*., 2016). The structure of the printed object also plays a crucial role in impact force reduction. One material that has been investigated for 3D printing is thermoplastic polyurethane (TPU), known for its flexibility and resilience.

One particularly intriguing type of structure is the honeycomb pattern, which mimics natural designs found in nature. The mechanical properties of honeycomb structures vary depending on the orientation of the printing angles. Previous studies have examined the impact force reduction of 3D-printed TPU honeycomb structures (Bates *et al*., 2016, 2019). However, the impact strength of these structures with different orientations has not been thoroughly investigated. Prior research has exclusively examined compressive stress in two structural orientations: transverse and ribbon. Ribbon structures have been observed to be more robust and absorb more energy than transverse structures (Bates *et al*., 2019; Habib, 2020). Moreover, there is an absence of research examining the effects that structural rotation has on impact force reduction. The mechanical properties of the structure are influenced by its density. An investigation has been conducted to determine the material's resistance to impact. However, the parameters evaluated differ in accordance with the particular application (Bates *et al*., 2019; Habib, 2020; Rahman *et al*., 2022; Rahman & Koohbor, 2020; Ramirez & Gupta, 2019). Therefore, previous research lacks information on the impact responses of honeycomb structures with different orientation angles and densities.

This study advances footwear industry knowledge of 3D printing and TPU designs. Thus, this study focused on understanding the honeycomb orientations and structure densities that minimize impact forces to enable the development of novel, high-performance footwear that emphasizes wearer health and comfort. The results can also be applied to other contexts that involve impact protection, such as hip protectors or lightweight helmets.

2. Materials and Methods

2.1. TPU properties and 3D printer

TPU (PolyFlex™ TPU95) was purchased from Palawatr Automation Co., Ltd. (Nakhon Pathom, Thailand). This TPU has 1.20 g/cm^3 density and 3-6 g melt index with 210 ºC, 1.2 kg. The mechanical properties of TPU are shown in Table 1. A three-dimensional custom printer was used in the experiment with the base size width $\times$ length $\times$ height equal to 200×200×200 millimeters, and nozzle size of 0.5 millimeters, with the printing resolution range 0.05-0.4 millimeters. The Ultimaker Cura 4.2.1 was used to generate G-code for printing. The conditions that were followed to 3D print TPU honeycombs are shown in Table 2.

Table 1. Mechanical properties of TPU

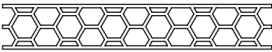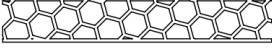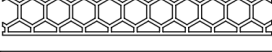| Property	Testing method	Typical value
100% modulus	ASTM-D638	9.4±0.3 (MPa)
Tensile strength	ASTM-D638	29.0±2.8 (MPa)
Elongation at break	ASTM-D638	330.1±14.9 (%)
Shore hardness	ASTM-D2240	95A
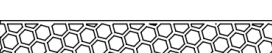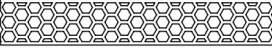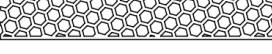
Table 2. The choices used in TPU printing

Parameter	Value
Print nozzle diameter (mm)	0.5
Nozzle temperature (˚C)	228
Build plate temperature (˚C)	50
Cooling fan	On
Printing speed (mm/s)	30
Print infill (%)	100
Raft separation distance (mm)	0.2
Retraction distance (mm)	1.0

2.2 3D printing design

Honeycomb pattern was designed with SolidWorks 2021 software from Applicad Public Company Limited. The wall thickness of 0.75 mm was kept the same with density in the range 0.24-0.48 g/cm^3, manipulated by varying wall-length between 1.80 and 3.54 mm. The honeycombs had three orientations of structure namely Ribbon (0ºC), Tran-Rib (15ºC) and Transverse (30ºC) as shown in Table 3. TPU honeycomb was printed in size 60 x 60 x10 mm. The determination of the relative density (ρ_{RD}) of a honeycomb structure can be achieved by employing the cell wall length l and thickness t. The relationship between the thickness and length of cells and their relative density is depicted in Equation 1. Furthermore, the ratio denoted as "t/l" is a component of a hexagonal unit cell. The equation provided represents the relative density of a hexagonal array in which the length varies while the wall thickness remains constant (Bates *et al*., 2019).

Table 3.   Honeycombs with different angle based on different density.

Case	Parameter	Angle (degrees)	Thickness and length (mm)	ρ_{RD}
Ribbon-0.24		0	t=0.75 l=3.54	0.24
Tran-Rib-0.24		15		
Transverse-0.24		30		
Ribbon-0.31		0	t=0.75 l=2.81	0.31
Tran-Rib-0.31		15		
Transverse-0.31		30		
Ribbon-0.36		0	t=0.75 l=2.38	0.36
Tran-Rib-0.36		15		
Transverse-0.36		30		
Ribbon-0.41		0	t=0.75 l=2.09	0.41
Tran-Rib-0.41		15		
Transverse-0.41		30		
Ribbon-0.48		0	t=0.75 l=1.80	0.48
Tran-Rib-0.48		15		
Transverse-0.48		30		
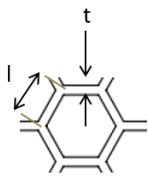
$$\rho_{RD} = \left(\frac{2}{\sqrt{3}}\right)\left(\frac{t}{l}\right) \quad (1)$$

2.3 Mechanical properties (compression tests)

The specimens' compressive properties were tested using an Instron 8872 from Instron (Thailand) equipped with a 25 kN loadcell. The square specimen had 50 mm length and 10 mm thickness. The testing machine compressed the specimens to 70% strain with a constant cross-head speed of 10 mm/min. This yielded a constant strain rate of 0.01 s^{-1}. The stress and strain relations were obtained from these tests.

2.4 Impact properties (drop test)

Shock absorption was evaluated in accordance with ASTM-F1614 using a custom-built drop-testing machine, shown in Figure 1. The thickness of the test specimens of molded samples was maintained at 10 mm. On each specimen, an 8.5 kg striker with a 45 mm diameter was dropped from 36 to 84 mm (corresponding to impact energies of 3–7 joules) [20–22]. The impact force was measured with a Kyowa Dengyo (Thailand) accelerometer, model ASH-A-100, and the specimen collapse distance was measured with a Kyowa Dengyo (Thailand) laser distance sensor, model AXIS-HP-200-1. The data were processed, recorded, and analyzed. The acceleration data were converted to impact forces by multiplying with the mass (8.5 kg). The impact acceleration values were used to calculate the impact cushioning efficiency (ICE) using Equation 2. The impact acceleration at solid TPU g_{max} was assessed on 100 % solid TPU, which denotes the complete printing of the TPU material, and Honeycomb g_{max}, which represents the impact acceleration values examined across a range of honeycomb structure types.
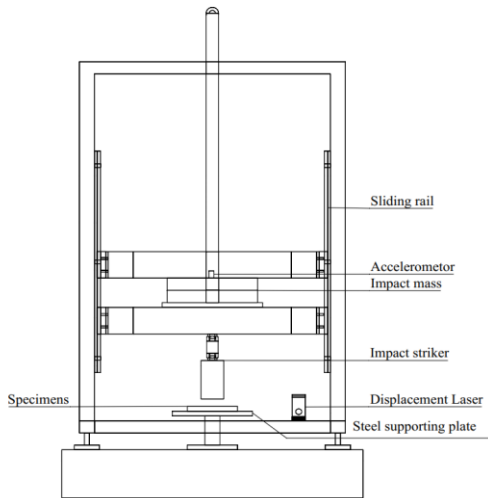
Figure 1. The custom-built drop-testing machine used to measure impact energy absorption

$$\text{Impact cushioning efficiency (ICE)} = \frac{\text{Solid TPU } g_{max} - \text{Honeycomb } g_{max}}{\text{Solid TPU } g_{max}} \quad (2)$$

3. Results and Discussion

3.1. Specimen quality

The Ultimaker Cura 4.3.0 software generated a G-code file to print the specimens. A controlled and consistent printing process was achieved at 30 mm/s. The specimens' infill structure was exact and detailed because of the 0.1 mm line pattern infill layer thickness. The material was printed at 228 °C to ensure effective printing. TPU flow and adhesion during printing are optimal at this temperature. To improve print adherence, the build plate was heated to 50 °C (Lopes *et al.*, 2018). This study used three samples per design and found consistent results (Basurto-Vázquez *et al.*, 2021). Every sample was of high quality and produced reliable test results.

Figure 2a shows vertically layered specimens with a 0.31 ρRD. Interior infill density is the amount of material used to fill the printed object. In this situation, 100% infill density maximizes specimen strength and density by creating a solid framework. The precise and consistent printing laid the groundwork for mechanical property research. Some of the specimens in Figure 2b are excellent. Table 4 lists these specimens' weight, size, and density. The specimens have the same 10 mm thickness, 60 mm width, and 60 mm length. Honeycomb structures with comparable relative density had similar physical properties in various orientations. A detailed study of the workpiece's size, weight, and dimensions shows an exceedingly small variance. These items with a higher relative density are heavier. Similar to prior investigations, honeycomb samples weighed 15–25 g and had a density of 0.4–0.70 g/cm³(Basurto-Vázquez *et al.*, 2021; Bates *et al.*, 2016, 2019).

3.2 Compression behavior of TPU honeycomb

Under the loading conditions depicted in Figure 3, the compressive forces of 3D printed TPU structures with
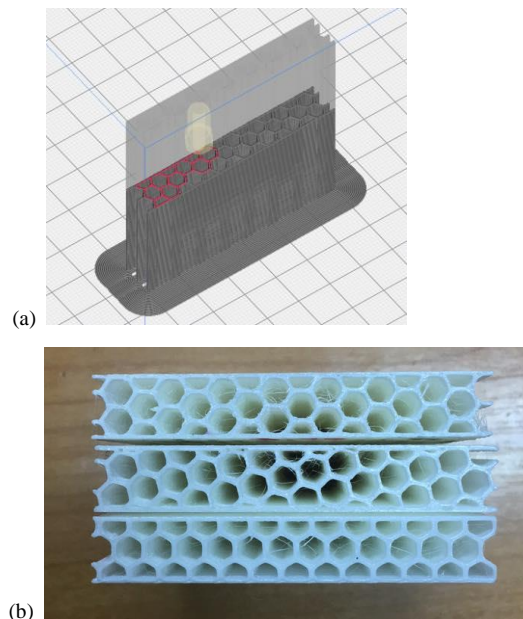

Figure 2. (a) The printing path of the honeycomb structure, (b) the TPU-printed honeycomb structure's quality (ρ_{RD} 0.31) in three different orientations (Top Ribbon, Middle Tran-Rib, and Bottom Transverse)

Table 4. Physical properties of 3D honeycomb printed structure

Case	Mass (g)	Thickness (mm)	Area (mm²)	Density (g/cm³)
Ribbon-0.24	15.4	9.80	3,555	0.44
Ribbon-0.31	17.2	9.60	3,579	0.50
Ribbon-0.36	20.0	9.85	3,597	0.56
Ribbon-0.41	21.4	9.85	3,570	0.61
Ribbon-0.48	23.9	9.80	3,633	0.67
Tran-Rib-0.24	15.6	10.00	3,570	0.44
Tran-Rib-0.31	17.7	9.90	3,606	0.50
Tran-Rib-0.36	19.7	9.90	3,606	0.55
Tran- Rib-0.41	21.5	9.90	3,591	0.60
Tran- Rib-0.48	23.8	10.00	3,618	0.66
Transverse-0.24	16.1	9.90	3,582	0.45
Transverse-0.31	17.3	9.90	3,564	0.49
Transverse-0.36	18.4	9.90	3,561	0.52
Transverse-0.41	21.7	9.80	3,594	0.62
Transverse-0.48	24.6	9.80	3,573	0.70
Solid TPU-100%	46.7	10.01	3,648	1.29

varying densities were evaluated. Each structure demonstrates three unique deformation stages: linear elasticity, plateau, and densification (Bates *et al.*, 2016, 2019; Li *et al.*, 2019). During initial compressive strains, the behavior is linear due to simple elastic resposes of the structure's cell walls. The cell walls buckle as deformation continues, culminating in the characteristic plateau phase. Densification occurs when the opposing cell walls eventually come into contact. The rigidity of the structure experiences a substantial increase during this densification phase, nearly reaching the stiffness of the initial solid material (Tomin & Kmetty, 2022).

Figure 3a initiates the comparison of 3D honeycomb structures at different densities by focusing on transversely
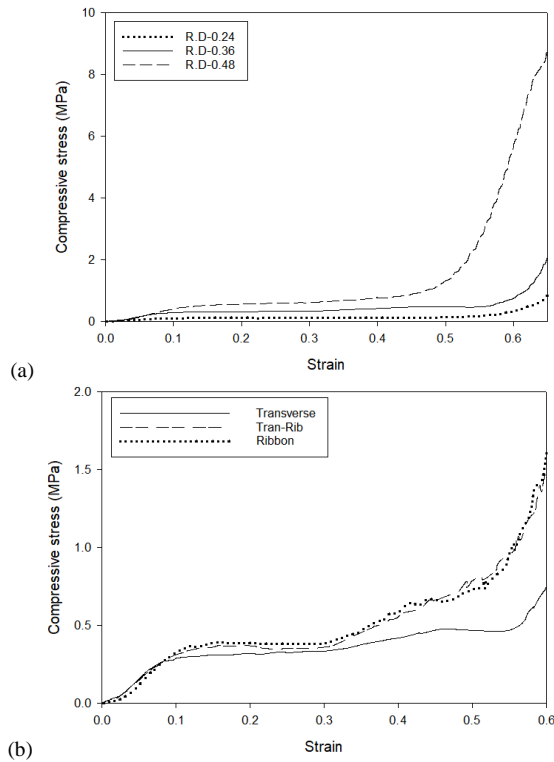
Figure 3. Stress-strain responses of three honeycombs structures printed from TPU (a) Transverse orientation with varied ρ_{RD}; and (b) ρ_{RD} = 0.36 with varied orientation angle

oriented honeycomb structures across three density levels. The results of this study agree with previous research that has examined the compressive properties of dense structures (Bates *et al.*, 2019; Tomin & Kmetty, 2022). Dense structures exhibit superior compressive characteristics. Notably, the high-density TPU 3D printing (RD 0.48) provides great structural strength. Furthermore, these structures exhibit exceptionally high energy adsorption capacities, as evidenced by the area under the stress-strain curve. This area increases with density of the structure. Due to their dimensions, structures with a high relative density have a reduced plateau stress range (Basurto-Vázquez *et al.*, 2021; Bates *et al.*, 2019; Rahman & Koohbor, 2020). As cellular dimensions decrease, there is a corresponding contraction of the intercellular space. So the distance at which densification occurs decreases in correlation with the relative density. Figure 3b demonstrates that altering the angle of the 3D structure affects its compressive properties. The results indicate that the compressive capacities of Ribbon and Tran-Rib structures are nearly identical, with ribbon angles being slightly more acute. On the other hand, the transverse structure with a trans angle exhibited the lowest compressive strength. Also, the transverse structure has a wider stress plateau than the other structures (Bates *et al.*, 2016, 2019; Habib, 2020). This means that the trans-angle structure can collapse more quickly than structures with other angles but with the same density. The observed differences in compression responses due to density variations and structural angles provide valuable insights for understanding the mechanical behavior of 3D-printed honeycomb structures.

Compressive strength characteristics varied with densities and angles in the honeycomb structures. Compressive stress increased with density, while structural angles affected compressive capacity. These findings help footwear product development by explaining cushioning-related mechanical features.

3.3 Dynamic behavior of TPU honeycomb (Force, time and displacement)

Impact tests conducted in accordance with ASTM-F1614 standard provide essential data about a material's or structure's response to impact (Srewaradachpisal *et al.*, 2020). The results usually include the impact value, which quantifies the force exerted during the impact, timing, and collapse distance, which measures how far the sample deforms or collapses under the impact force. ASTM-F1614 ensures consistency and reliability when evaluating materials and products. A small impact force indicates effective impact absorption, while the collapse distance indicates how much the material or product must bend to absorb impact energy.

Figure 4a illustrates the impact attenuation test results of the workpieces having different relative densities. The Solid TPU 100% demonstrates the highest impact force and the least amount of cushioning. Obviously, although the workpieces possess the same honeycomb structure, density of the sample significantly affected the impact attenuation. Here, the displacement decreased with density. The samples (RD-0.24 and RD-0.48) still had high impact force, indicating low shock absorption. The medium relative density (RD-0.36) showed the lowest impact force, indicating high absorption of the impact energy. The observed variations in impact behavior among the samples can be linked to their distinct mechanical properties, as illustrated in Figure 3a in comparison to Figure 4b. Sample RD-0.36 collapsed within a plateau region, similar to RD-0.48, which also experienced plateau collapse but at a higher force due to its strong structure. RD-0.24 collapsed within a densification region, surpassing the plateau stress region. Comparatively, research on the impact force of honeycomb structures yields consistent results indicating that the impact reduction is influenced differently in different density ranges of honeycomb structures (Bates *et al.*, 2019). This variation can be attributed to the distinct mechanical properties of the honeycomb structures (Srewaradachpisal *et al.*, 2020). In order to ascertain the optimal density of structure for implementation in practical contexts, experimentation is therefore necessary (Rahman *et al.*, 2022). The selection of an optimal density gradient may be necessary in applications that demand a wide range of impact energies, dependent upon the specific design criteria and application at hand (Bates *et al.*, 2019; Rahman *et al.*, 2022; Rahman & Koohbor, 2020).

Figure 4c illustrates the impact attenuation test results of the workpieces having different orientation angle of structures. It was found that the orientation angle had a slight effect on the impact attenuation. The study revealed that structures oriented at transverse angles demonstrated the most effective reduction in impact forces. Additionally, within this density range, Ribbon and Rib-Tran angles exhibited comparable abilities to decrease forces. This observation aligns with the compressive properties depicted in Figure 3b, where Ribbon and Rib-Tran structures displayed similar
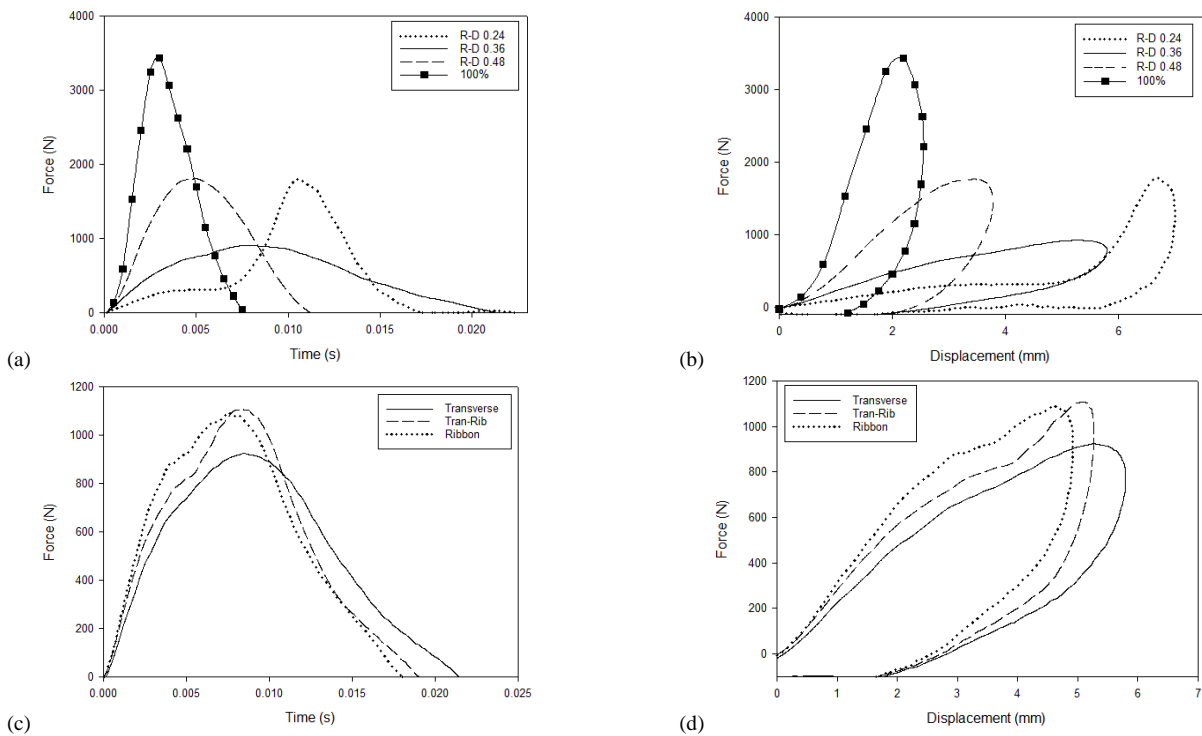
Figure 4. Drop test results for TPU honeycombs having transverse orientation with varied ρ_{RD}: (a) force vs time, (b) force vs displacement. Cases with $\rho_{RD} = 0.36$ and varied orientation angle: (c) force vs time, and (d) force vs displacement

mechanical characteristics. Previous research was solely concerned with comparing the mechanical properties of ribbon and transverse honeycomb structures (Bates *et al.*, 2016, 2019). This current study has thus revealed distinctions in the impact characteristics of structures oriented at various angles that were previously unknown. Among them, the sample with transverse angle undergoes the largest displacement in Figure 4d. As compared to the relative density of samples, it is clear that the orientation angle showed less effect on the impact properties.

3.4 Dynamic behavior at varied impact energies

Spline curve graphs were used to evaluate structures with 3–7 joules of impact energy. Throughout the testing, these graphs showed the relationship between impact force, collapse distance (displacement), and structural relative density. These results highlight the importance of optimizing structure density to absorb impact forces within the prescribed energy range. Figure 5 shows the importance of density customization in designing and developing structures that can absorb impact forces in the prescribed test energy range.

Upon examining the honeycomb structures under various impact energy levels, as shown in Figures 5a, 5c, and 5e for transverse, trans-rib, and ribbon orientations respectively, it is evident that higher impact energies led to increased impact forces (Bates *et al.*, 2019; Ramirez & Gupta, 2019; Srewaradachpisal *et al.*, 2020). The study identified optimal densities that effectively minimized these impact forces: 0.31, 0.36, and 0.41 for transverse structures. For trans-rib structures, the most efficient densities by impact energy levels were 0.31-0.36, 0.36, and 0.41, respectively.

Similarly, for ribbon structures, the most effective densities were consistently found to be about 0.36 across impact energies of 3, 5, and 7 joules. Different structural orientations had different densities that were effective in reducing impact forces. Furthermore, different impact energies also lead to different optimal densities for efficient impact reduction.

When considering the collapse distances (displacement) of the structures under impact, as illustrated in Figures 5b, 5d, and 5f, it was observed that at the same impact energy level, structures with lower density experienced greater collapse distances compared to those with higher density (Ramirez & Gupta, 2019). Besides, it was evident that higher impact energies led to greater collapse distances (displacement). Upon examining all figures, it becomes evident that the reduction in impact force is directly related to the collapse distance. Structures that collapse more can effectively mitigate impact forces. However, if the structure's density is excessively low, it might collapse significantly and fail to absorb the impact force effectively, being unable to accommodate the energy. In such cases, the structure collapses into the plateau stress region and transitions into the densification phase, akin to the behavior observed in Figure 4a. These findings demonstrate the complicated relationship between impact energy, structural density, and collapse distance, contributing to the design and optimization of honeycomb structures to absorb impact forces at varied energy levels.

Figure 6 displays the results from impact tests conducted within the 3-7 joule range of impact energy. These results are compared to the relative density of honeycomb structures at different angles. As depicted in Figure 6a, it is noticeable that, at an impact energy level of 3 joules, the
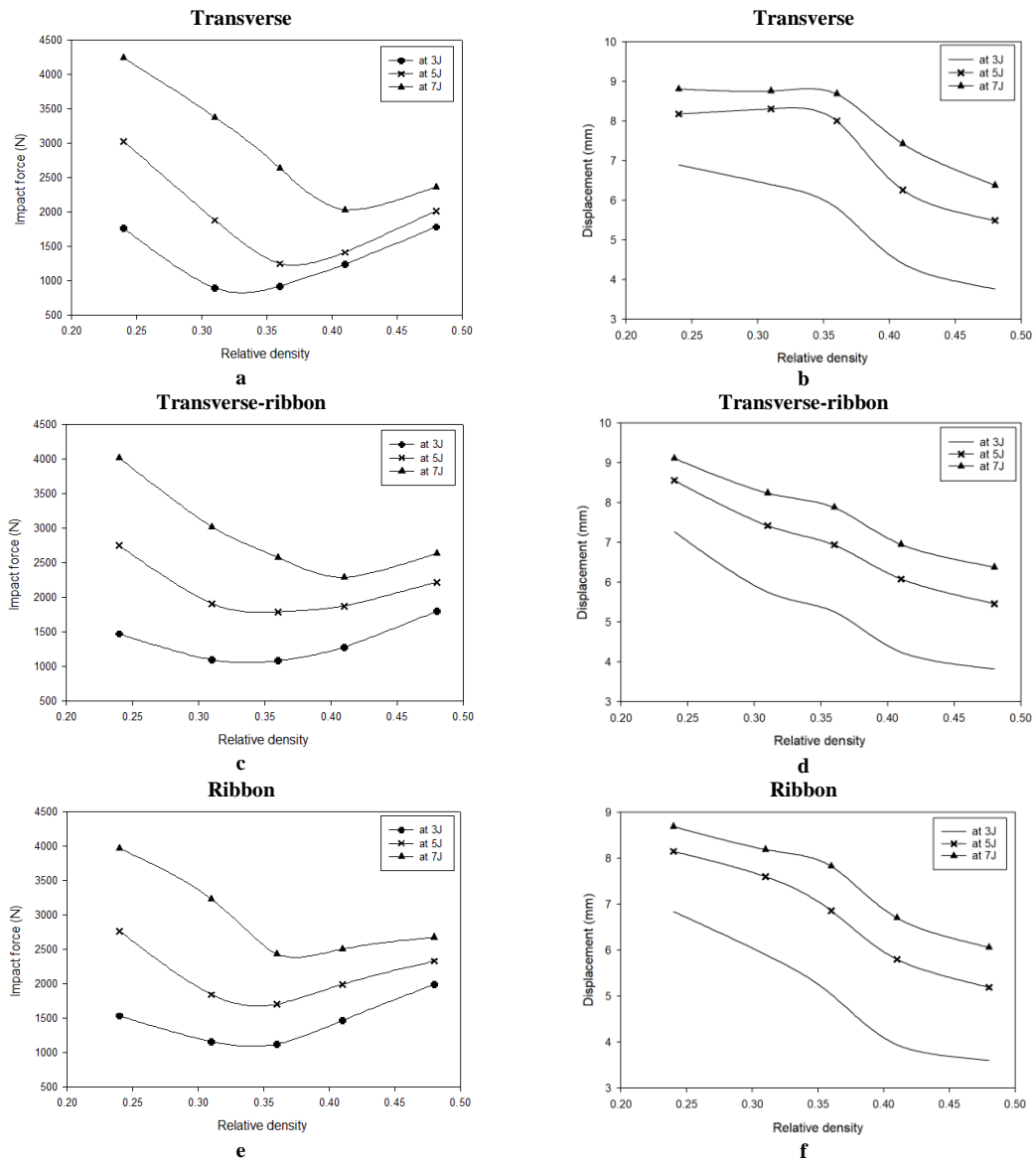
Figure 5.   The impact of honeycomb structure orientation when energy is manipulated. (a) The transverse impact force versus relative density (ρ_{RD}). (b) Transverse displacement in relation to ρ_{RD}. (c) Trans-rib impact force versus ρ_{RD}. (d) Trans-rib displacement concerning ρ_{RD}. (e) Ribbon impact force versus ρ_{RD}. (f) Ribbon displacement versus ρ_{RD}.

transverse, ribbon, and trans-rib honeycomb structures demonstrated superior damping performance at relative densities within the range of 0.31-0.36 similarly. Notably, among these structures, the transverse design clearly outperforms others in reducing loads.

In Figure 6b, the impact cushioning efficiency comparing solid TPU is demonstrated. The analysis reveals that different structural designs led to varying impact absorption efficiencies. Transversely oriented structures reduced impact better than the other structures, with an efficiency of 0.75 compared to 0.65. Less dense materials absorb shock better than denser ones, with 0.48–0.58 and 0.42–0.48 efficiencies, respectively. At this impact energy, lower densities absorb impact better than higher densities.

Figure 6c shows that impact forces at 5 joules of impact energy followed the same patterns as at 3 joules. Transversely oriented structures reduced impact effectively. The optimal density for impact reductions remained 0.36. In Figure 6d, transverse structures at 0.36 density had a greater impact reduction efficiency of 0.75 than the other structures at 0.6. It has become apparent that higher densities in this energy range are more efficient in impact reduction compared to lower density ranges.

In Figure 6e, similar to previous observations, the transversely oriented structures continue to demonstrate the best impact reduction capabilities within the density range of 0.41. Figure 6f illustrates the diminishing impact reduction
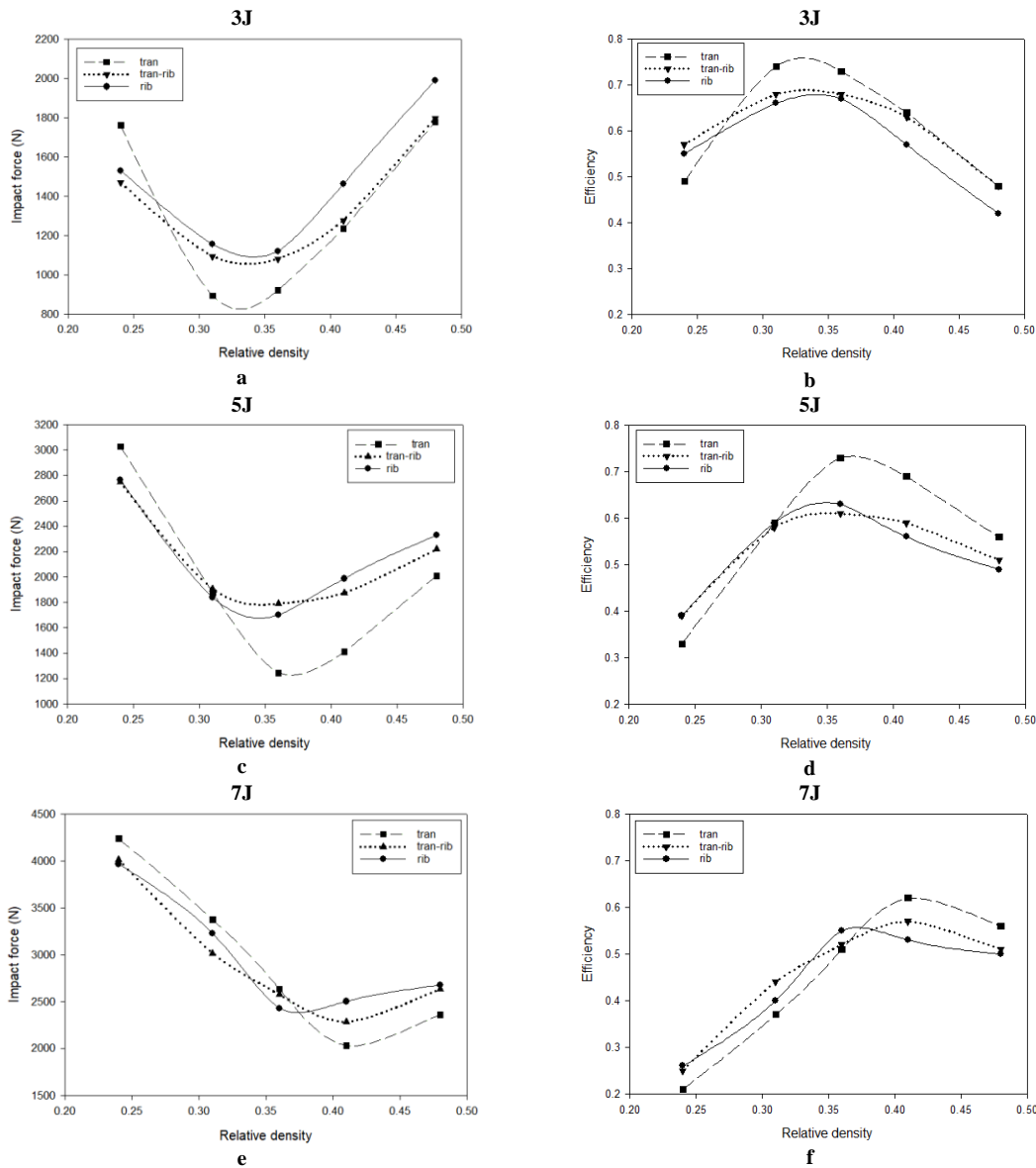
Figure 6.   The impact of honeycomb structure orientation is detailed at specific energy levels: (a) 3 J, impact force vs ρ_{RD}, (b) 3 J, displacement vs ρ_{RD}, (c) 5 J, impact force vs ρ_{RD}, (d) 5 J, displacement vs ρ_{RD}, € 7 J, impact force vs ρ_{RD}, and (f) 7 J displacement vs ρ_{RD}.

efficiency. In this scenario, transverse structures maintain their superior impact reduction efficiency, scoring 0.62, while the other designs only achieve an efficiency level of 0.55 at this specific impact energy level. Additionally, it becomes evident that higher density ranges exhibit better impact reduction capabilities compared to lower density ranges.

4. Conclusions

In this research, it was discovered that the honeycomb structure with a transverse orientation demonstrated superior impact reduction capabilities across all energy of impact scenarios. Regarding the trans-rib and ribbon orientations, they exhibited similar impact attenuation. Notably, this configuration boasted the lowest density, making it an excellent choice for manufacturing lightweight impact resistant components. Additionally, it incurred lower production expenses compared to the high-density counterparts. The experiments indicated that low-density structures proved more efficient at mitigating impacts under low impact energy conditions. Conversely, high-density structures proved more effective in absorbing impacts during high impact energy scenarios. As a result, structure density should be prioritized over structure orientation when choosing a honeycomb for shock absorption.

Acknowledgements

References

Basurto-Vázquez, O., Sánchez-Rodríguez, E. P., McShane, G. J., & Medina, D. I. (2021). Load distribution on pet-g 3d prints of honeycomb cellular structures under compression load. *Polymers*, *13*(12), 1–13. Retrieved from https://doi.org/10.3390/polym1312 1983

Bates, S. R. G., Farrow, I. R., & Trask, R. S. (2016). 3D printed polyurethane honeycombs for repeated tailored energy absorption. *Materials and Design*, *112*, 172–183. Retrieved from https://doi.org/10.1016/j.matdes.2016.08.062

Bates, S. R. G., Farrow, I. R., & Trask, R. S. (2019). Compressive behaviour of 3D printed thermoplastic polyurethane honeycombs with graded densities. *Materials and Design*, *162*, 130–142. Retrieved from https://doi.org/10.1016/j.matdes.2018.11.019

Brückner, K., Odenwald, S., Schwanitz, S., Heidenfelder, J., & Milani, T. (2010). Polyurethane-foam midsoles in running shoes - Impact energy and damping. *Procedia Engineering*, *2*(2), 2789–2793. Retrieved from https://doi.org/10.1016/j.proeng.2010.04.067

Dib, M. Y., Smith, J., Bernhardt, K. A., Kaufman, K. R., & Miles, K. A. (2005). Effect of environmental temperature on shock absorption properties of running shoes. *Clinical Journal of Sport Medicine*, *15*(3), 172–176. Retrieved from https://doi.org/10.1097/01.jsm.0000165348.32767.32

Habib, F. N. (2020). *Development of high performing 3D printed polymeric cellular structures for wearable impact protection* (Issue July). Melbourne, Australia: School of Engineering, Faculty of Science, Engineering and Technology Swinburne University of Technology Melbourne, Australia.

Heidenfelder, J., Sterzing, T., & Milani, T. L. (2009). Biomechanical wear testing of running shoes. *Footwear Science*, *1*(September 2016), 16–17. Retrieved from https://doi.org/10.1080/194242809 02977046

Li, D., Liao, W., Dai, N., & Xie, Y. M. (2019). *Absorption of sheet-based and strut-based Gyroid*.

Lippa, N., Hall, E., Piland, S., Gould, T., & Rawlins, J. (2014). Mechanical ageing protocol selection affects macroscopic performance and molecular level properties of ethylene vinyl acetate (EVA) running shoe midsole foam. *Procedia Engineering*, *72*(Mills 2007), 285–291. Retrieved from https://doi.org/10.1016/j.proeng.2014.06.082

Lopes, L. R., Silva, A. F., & Carneiro, O. S. (2018). Multi-material 3D printing: The relevance of materials affinity on the boundary interface performance. *Additive Manufacturing*, *23*(March), 45–52. Retrieved from https://doi.org/10.1016/j.addma.2018.06.027

Mercer, J. A., & Horsch, S. (2015). Heel-toe running: A new look at the influence of foot strike pattern on impact force. *Journal of Exercise Science and Fitness*, *13*(1), 29–34. Retrieved from https://doi.org/10.1016/j.jesf.2014.12.001

O'Leary, K., Vorpahl, K. A., & Heiderscheit, B. (2008). Effect of cushioned insoles on impact forces during running. *Journal of the American Podiatric Medical Association*, *98*(1), 36–41. Retrieved from https://doi.org/10.7547/0980036

Price, C., Cooper, G., Graham-Smith, P., & Jones, R. (2014). A mechanical protocol to replicate impact in walking footwear. *Gait and Posture*, *40*(1), 26–31. Retrieved from https://doi.org/10.1016/j.gaitpost.2014.01.014

Rahman, O., & Koohbor, B. (2020). Optimization of energy absorption performance of polymer honeycombs by density gradation. *Composites Part C*: *Open Access*, *3*(August), 100052. Retrieved from https://doi.org/10.1016/j.jcomc.2020.100052

Rahman, O., Uddin, K. Z., Muthulingam, J., Youssef, G., Shen, C., & Koohbor, B. (2022). Density-graded cellular solids: Mechanics, fabrication, and applications. *Advanced Engineering Materials*, *24*(1), 1–20. Retrieved from https://doi.org/10.1002/adem.202100646

Ramirez, B. J., & Gupta, V. (2019). Energy absorption and low velocity impact response of open-cell polyurea foams. *Journal of Dynamic Behavior of Materials*, *5*(2), 132–142. Retrieved from https://doi.org/10.1007/s40870-019-00192-0

Silva, R. M., Rodrigues, J. L., Pinto, V. V., Ferreira, M. J., Russo, R., & Pereira, C. M. (2009). Evaluation of shock absorption properties of rubber materials regarding footwear applications. *Polymer Testing*, *28*(6), 642–647. Retrieved from https://doi.org/10.1016/j.polymertesting.2009.05.007

Speed, G., Harris, K., & Keegel, T. (2018). The effect of cushioning materials on musculoskeletal discomfort and fatigue during prolonged standing at work: A systematic review. *Applied Ergonomics*, *70*(February), 300–314. Retrieved from https://doi.org/10.1016/j.apergo.2018.02.021

Srewaradachpisal, S., Dechwayukul, C., Chatpun, S., Spontak, R. J., & Thongruang, W. (2020). Optimization of the rubber formulation for footwear applications from the response surface method. *Polymers*, *12*(9), 7–11. Retrieved from https://doi.org/10.3390/POLYM12092032

Tomin, M., & Kmetty, Á. (2022). Polymer foams as advanced energy absorbing materials for sports applications—A review. *Journal of Applied Polymer Science*, *139*(9), 1–23. Retrieved from https://doi.org/10.1002/app.51714

Verdejo, R., & Mills, N. J. (2004). Heel-shoe interactions and the durability of EVA foam running-shoe midsoles. *Journal of Biomechanics*, *37*(9), 1379–1386. Retrieved from https://doi.org/10.1016/j.jbiomech.2003.12.022